JOURNAL OF AIRCRAFT
Vol. 48, No. 2, March–April 2011

Estimation of Turbulent Vertical Velocity from Nonlinear Simulations of Aircraft Response

Donglong Sheu* and Chuan-Tau Lan†
National Cheng Kung University, Tainan 70101, Taiwan, Republic of China

DOI: 10.2514/1.C031190

The objective of this paper is to estimate the unknown vertical velocity component of atmospheric turbulence on a transport aircraft based on data in the flight data recorder with accuracy consistent with the measurement of the alpha sensor. Such vertical velocity component of low frequency (to be called the wind) is not measurable quantitatively with the existing onboard weather radars. The idea is to estimate the vertical wind speed from aircraft response by integrating the nonlinear flight dynamic equations. The motivation of developing this new approach arises from flight trajectory reconstruction of a transport aircraft in an accident with the aerodynamics being unsteady and nonlinear. Because the conventional forward integration with a Runge–Kutta fourth-order scheme tends to diverge, in particular in the predicted altitude, an innovative approach which can maintain the accuracy of numerical integration over a long time period for a system of implicit nonlinear flight dynamic equations is introduced in this paper. The new approach is to add and subtract a linear part of the nonlinear differential equations, with one term being treated implicitly (i.e., unknown) and the other term, together with the other aerodynamic forces and moments, being known function of time. This implicit linear part serves as the numerical damping that reduces or eliminates the growth of errors in numerical forward integrations. Application to a transport aircraft in severe turbulence encounter is illustrated.

Nomenclature

g	=	gravity acceleration
I_{xx}, I_{yy}, I_{zz}, I_{xz}	=	components of moments of inertia
k_1, k_2	=	reduced frequencies based on the variation of angles of attack and roll angles, respectively
m	=	mass
p, q, r	=	roll rate, pitch rate, yaw rate, respectively
t	=	time
u, v, w	=	components of inertial velocity in aircraft body axes
V	=	inertial velocity
V_a	=	airspeed
X, Y, Z	=	components of total force in body frame
x_e, y_e, z_e	=	components of position vectors in earth frame
α	=	angle of attack
β	=	sideslip angle
δ	=	control surface deflection
θ, ϕ, ψ	=	pitch angle, bank angle, heading angle

Subscripts

a	=	aileron
e	=	elevator
m	=	due to motion
r	=	rudder
t	=	total
w	=	due to wind
0	=	initial value

Received 23 July 2010; revision received 1 November 2010; accepted for publication 2 November 2010.

*Associate Professor, Department of Aeronautical and Astronautical Engineering. Senior Member AIAA.

†J. L. Constant Distinguished Professor Emeritus, The University of Kansas. Currently, Visiting Professor, Department of Aeronautical and Astronautical Engineering. Associate Fellow AIAA.

Introduction

ESTIMATION of atmospheric turbulence field encountered by aircraft continues to be an interesting problem. In meteorology, turbulence has long represented one of the most demanding conceptual and forecasting challenges due to its fine spatial and temporal scale [1]. In numerical meteorology, wind with horizontal dimensions ranging from around five to several hundred kilometers can be resolved adequately. However, to accurately diagnose aircraft normal load accelerations, resolved scales of motion as small as 50 m are needed [2]. In fact, spatial resolution should be well below the aircraft length of which the order is 30 m [3].

From another point of view, an aircraft itself is in fact a big sensor in the atmospheric environment. Penetrating a turbulent air zone, the aircraft responds in a definite way depending on the imposed wind field and aircraft aerodynamic characteristics. Therefore, from the response the input including the turbulence can be identified. As the atmospheric turbulence is random in nature, it is composed of a wide spectrum of frequencies. Therefore, the response data can only provide the estimation of the significant components of the low-frequency part of atmospheric turbulence, to be called the wind. With this concept, Stewart [4] described a normal force in situ turbulence algorithm, which assumes the normal force coefficient is primarily dependent linearly on the angle of attack with much smaller contributions from other parameters such as the elevator and pitch rate. The aerodynamics used is from the database of flight simulators for normal flights.

While in [4], the algorithm can produce information that can be used to predict hazardous accelerations of airplanes or to aid meteorologists in forecasting weather patterns, the aerodynamic models are based on the design data which are suitable only for normal flight conditions. Buck et al. [5] estimated the aircraft response based on linear flight dynamic equations in pitch and plunge with aircraft aerodynamics derived again from normal flight conditions and the imposed turbulent field from flight test. Stuever [6] found that by a forward integration of the plunging equation in the nonlinear form, the results in altitude variation diverged quickly. The integration would converge only if the linear part in lift curve slope was factored out and treated as an implicit part of the nonlinear differential equations.

In this paper, Stuever's [6] idea will be extended to integrating the general nonlinear flight dynamic equations in six degrees of freedom. The aerodynamic models are constructed by using the fuzzy logic algorithm [7,8] based on the data in the flight data recorder (FDR) for an aircraft encountering severe atmospheric turbulence. The objective of this paper is to use the FDR data of a jet transport aircraft to estimate the vertical velocity component of turbulent air from the aircraft response. The airplane is subjected to the estimated total forces and moments at measured angles of attack that include the atmospheric turbulence. The angle of attack measurement is in one point per second (1 Hz); while the normal acceleration, or the normal force coefficient, is in eight points per second (8 Hz). While the data resolution may not be high enough for turbulence in all frequencies, it should be sufficient to estimate the turbulence components at lower frequencies of interest to flight dynamics. The idea is to obtain the angle of attack due to motion through integration of the dynamic equations of motion, and subtract it from the total measured values to arrive at the vertical velocity component of turbulence.

In integrating the equations involving fast-varying variables in turbulence encounter, one numerical problem is that there is no explicit damping term in the equations. The problem has been solved in this paper by isolating the term associated with the first derivative. A numerical example with a set of FDR data of a jet transport aircraft is given to illustrate the prediction of turbulence vertical wind.

Theoretical Formulation

In trajectory reconstruction, the flight dynamic equations to be integrated are assumed to be as follows:

$$\frac{\mathrm{d}V}{\mathrm{d}t} = \left(\frac{X}{m} - g\sin\theta\right)\cos\alpha\cos\beta + \left(\frac{Y}{m} + g\cos\theta\sin\phi\right)\sin\beta + \left(\frac{Z}{m} + g\cos\theta\cos\phi\right)\sin\alpha\cos\beta \tag{1}$$

$$\frac{\mathrm{d}\alpha}{\mathrm{d}t} = \left\{\left[\frac{1}{V}\left(-\frac{X}{m} + g\sin\theta\right) - r\sin\beta\right]\sin\alpha + \left[\frac{1}{V}\left(\frac{Z}{m} + g\cos\theta\cos\phi\right) - p\sin\beta\right]\cos\alpha\right\}\frac{1}{\cos\beta} + q \tag{2}$$

$$\frac{\mathrm{d}\beta}{\mathrm{d}t} = \left[-\left(\frac{X}{m} - g\sin\theta\right)\frac{\sin\beta}{V} - r\right]\cos\alpha + \left(\frac{Y}{m} + g\cos\phi\sin\phi\right)\frac{\cos\beta}{V} + \left[-\left(\frac{Z}{m} + g\cos\theta\cos\phi\right)\frac{\sin\beta}{V} + p\right]\sin\alpha \tag{3}$$

$$\frac{\mathrm{d}p}{\mathrm{d}t} = \left[L + \frac{I_{xz}N}{I_{zz}} + I_{xz}\left(1 + \frac{I_{xx} - I_{yy}}{I_{zz}}\right)pq + \left(I_{yy} - I_{zz} - \frac{I_{xz}^2}{I_{zz}}\right)qr\right]\frac{1}{AI_{xx}} \tag{4}$$

$$\frac{\mathrm{d}q}{\mathrm{d}t} = [M + I_{xz}(r^2 - p^2) + (I_{zz} - I_{xx})rp]\frac{1}{I_{yy}} \tag{5}$$

$$\frac{\mathrm{d}r}{\mathrm{d}t} = \left[\frac{I_{xz}L}{I_{xx}} + N + \left(I_{xx} - I_{yy} + \frac{I_{xz}^2}{I_{xx}}\right)pq + \left(\frac{I_{yy} - I_{zz}}{I_{xx}} - 1\right)I_{xz}qr\right]\frac{1}{AI_{zz}} \tag{6}$$

where $A \triangleq 1 - I_{xz}^2/(I_{xx}I_{zz})$

The kinematic equations are:

$$\frac{\mathrm{d}\theta}{\mathrm{d}t} = q\cos\phi - r\sin\phi \tag{7}$$

$$\frac{\mathrm{d}\phi}{\mathrm{d}t} = p + \tan\theta(q\sin\phi + r\cos\phi) \tag{8}$$

$$\frac{\mathrm{d}\psi}{\mathrm{d}t} = (q\sin\phi + r\cos\phi)\sec\theta \tag{9}$$

In Eqs. (1–6), aerodynamic forces and moments based on body-fixed axes, X, Y, Z, L, M, N, can be estimated from the fuzzy logic aerodynamic models. But for the present application, the aerodynamic coefficients are directly obtained as results of bias analysis.

Results from integration based on the body-fixed axes are to be integrated for the trajectory (x, y, z) based on ground-fixed axes by using the following equations:

$$\frac{\mathrm{d}x_e}{\mathrm{d}t} = u\cos\theta\cos\psi + v(\sin\phi\sin\theta\cos\psi - \cos\phi\sin\psi) + w(\cos\phi\sin\theta\cos\psi + \sin\phi\sin\psi) \tag{10}$$

$$\frac{\mathrm{d}y_e}{\mathrm{d}t} = u\cos\theta\sin\psi + v(\sin\phi\sin\theta\sin\psi + \cos\phi\cos\psi) + w(\cos\phi\sin\theta\sin\psi - \sin\phi\cos\psi) \tag{11}$$

$$\frac{\mathrm{d}z_e}{\mathrm{d}t} = -u\sin\theta + v\sin\phi\cos\theta + w\cos\phi\cos\theta \tag{12}$$

where the velocity components (u, v, w) based on the body axes are the aircraft inertial speed components and are given by:

$$u = V\cos\beta_t\cos\alpha_t \tag{13}$$

$$v = V\sin\beta_t \tag{14}$$

$$w = V\cos\beta_t\sin\alpha_t \tag{15}$$

The initial conditions are all provided by the FDR data as well as estimated variables in the bias analysis. Note that in the usual form of Eqs. (13–15), the (u, v, w)-components are due to motion only and do not include the effects of external wind. In other words, here we have to use the velocity components relative to the ground in the final integration. One way to achieve this is to replace α and β in Eqs. (13–15) by α_t (or α_{total}), and β_t; where

$$\alpha_t = \alpha_m + \alpha_w \tag{16}$$

$$\beta_t = \beta_m + \beta_w \tag{17}$$

where the subscript m stands for motion, and w for wind; α_m and β_m are obtained directly from integrating the flight dynamic equations. What we need are, therefore, α_w and β_w. In the FDR, we usually have the data on ground speed and drift angle, and/or wind speed and wind direction. From these, we can estimate the crosswind and wind speed along the flight path, all roughly on the horizontal plane. Therefore, β_w is known when an aircraft does not roll. In general, the crosswind must be rotated into the local body-fixed coordinate system to obtain the final values of angle of attack and sideslip angle due to crosswind, α_{w_1} and β_{w_1} [9]. What remains to be estimated is the effect of turbulent vertical speed (α_{w_2}). Note that total α is measured by the α-vane (i.e., the α-sensor). Therefore

$$\alpha_{w_2} = \alpha_{\mathrm{total}} - \alpha_m - \alpha_{w_1} \tag{18}$$

The vertical velocity is then given by

$$V_w = V_a\alpha_{w_2}/(\cos\theta\cos\phi) \tag{19}$$

where V_w is normal to the horizontal plane and V_a is the airspeed. Note that we will ignore the turbulent effects on engine thrust and hence on u, since turbulent effects on engine thrust are not known. Therefore, to estimate the vertical velocity components of turbulence, we have to integrate the equations of motion for α_m. Numerical solutions of differential equations involve two issues: the first one being numerical stability and the second one being numerical accuracy. In integrating the flight dynamic equations involving fast-varying variables in turbulence encounter, difficulty is encountered in the numerical stability in that there is no damping term in the linear part of the equations, as indicated earlier. To resolve this difficulty, Eq. (2) is recast into the following form:

$$\frac{\mathrm{d}\alpha}{\mathrm{d}t} - f_{1_\alpha}\alpha = f_1(t, x_i) - f_{1_\alpha}\alpha = g(t, x_i) \tag{20}$$

where f_1 is equal to the right-hand side of Eq. (2). In other words, the term associated with the first derivative is isolated. If the first derivative is negative, Eq. (20) should be adjusted accordingly. In addition, there is a term associated with $\mathrm{d}\alpha/\mathrm{d}t$ in the aerodynamic forces. This should be factored out as well. Then Eq. (20) becomes:

$$\frac{\mathrm{d}\alpha}{\mathrm{d}t}(1 - Z_{\dot{\alpha}}) - f_{1_\alpha}\alpha = f_1(t, x_i) - f_{1_\alpha}\alpha - Z_{\dot{\alpha}}\dot{\alpha} = g_{11}(t, x_i)$$

or

$$\frac{\mathrm{d}\alpha}{\mathrm{d}t} - \frac{f_{1_\alpha}}{1 - Z_{\dot{\alpha}}}\alpha = \frac{g_{11}(t, x_i)}{1 - Z_{\dot{\alpha}}} = g_{12}(t, x_i) \tag{21}$$

where

$$Z_{\dot{\alpha}} = \frac{\bar{q}S}{Vm}\frac{\bar{c}}{2V}(-C_{x_{\dot{\alpha}}}\sin\alpha + C_{z_{\dot{\alpha}}}\cos\alpha)/\cos\beta \tag{22}$$

Because $mV\mathrm{d}\alpha/\mathrm{d}t$ is the inertial force, $Z_{\dot{\alpha}}$ represents the virtual mass in unsteady aerodynamics. The virtual mass may significantly affect the motion as the aircraft mass does. Therefore, it is important to combine it with the physical mass term. Usually, this term is small. But in atmospheric turbulence it may be of the order of unity in magnitude. If it is large and positive, it will create numerical problem in Eq. (21). In this case, the other term being subtracted on the right-hand side should be moved to the left-hand side. Note that the first derivative is generally a function of time. In numerical integration, the f_{1_α}-term is treated as an implicit term and the g_{12}-term is an explicit function of t. The left-hand side of Eq. (21) can be written as a total derivative of (αP) such that

$$\frac{1}{P}\frac{\mathrm{d}(\alpha P)}{\mathrm{d}t} = g_{12}(t, x_i) \tag{23}$$

where P can be obtained based on the concept of integrating factor in calculus as:

$$P = \exp\left\{-\int_{t_0}^{t}\frac{f_{1_\alpha}}{1 - Z_{\dot{\alpha}}}\,\mathrm{d}t\right\} \tag{24}$$

Therefore, Eq. (2) is now modified to be:

$$\frac{\mathrm{d}(\alpha P)}{\mathrm{d}t} = Pg_{12}(t, x_i) = F(t, x_i) \tag{25}$$

Equation (25) can be integrated with any reliable numerical scheme. In the present application, it is integrated with a fourth-order Runge–Kutta scheme. Integration of Eq. (25) is found to be quite stable. Similarly, the same concept is applied to the $\mathrm{d}\beta/\mathrm{d}t$-equation. The resulting equation is similar to Eq. (21):

$$\frac{\mathrm{d}\beta}{\mathrm{d}t} - \frac{f_{2_\beta}}{1 - Y_{\dot{\beta}}}\beta = \frac{g_{21}(t, x_i)}{1 - Y_{\dot{\beta}}} = g_{22}(t, x_i) \tag{26}$$

where f_2 is equal to the right-hand side of Eq. (3) and

$$Y_{\dot{\beta}} = \frac{\bar{q}S}{mV}\frac{b}{2V}C_{y_{\dot{\beta}}}\cos\beta \tag{27}$$

On the other hand, Eq. (12) is modified to be:

$$\frac{\mathrm{d}z_e}{\mathrm{d}t} = -u\sin\theta + v\sin\phi\cos\theta + w\cos\phi\cos\theta + k_g(z_e - z_{\mathrm{ref}}) - k_g(z_e - z_{\mathrm{ref}}) \tag{28}$$

where the "gain" constant, k_g, is set to 10 based on numerical experimentation. Since z_e is negative, Eq. (27) should be written as

$$\frac{\mathrm{d}z_e}{\mathrm{d}t} - k_g(z_e - z_{\mathrm{ref}}) = -u\sin\theta + v\sin\phi\cos\theta + w\cos\phi\cos\theta \tag{29}$$

Setting the LHS of Eq. (29) as:

$$\frac{\mathrm{d}z_e}{\mathrm{d}t} - k_g(z_e - z_{\mathrm{ref}}) = \frac{1}{P}\frac{\mathrm{d}(z_e P)}{\mathrm{d}t}$$

we can show that

$$\frac{\dot{P}}{P} = -k_g\left(1 - \frac{z_{\mathrm{ref}}}{z_e}\right)$$

It follows that

$$P = \exp\left\{-k_g\int_{t_0}^{t}\left(1 - \frac{z_{\mathrm{ref}}}{z_e}\right)\mathrm{d}t\right\}$$

Large damping can be obtained if we set z_{ref} in the above equation to zero. Maintaining a correct altitude is important in determining the air density and hence the correct aerodynamic forces and moments. Therefore

$$P = \exp\left\{-k_g\int_{t_0}^{t}\mathrm{d}t\right\} \tag{30}$$

P in Eq. (30) tends to become very small quickly. If it is less than 10^{-10}, it is set to 10^{-10}. Similarly, for the y_e-equation [Eq. (11)], a term $-C_2 y_e$ is added to both sides of Eq. (11). C_2 is taken to be 2.0. Without it, y_e would diverge. Numerical results indicate that all other equations do not have the difficulty in numerical stability, perhaps because the main independent variables, α_m, β_m, and altitude, for the aerodynamic forces and moments are now numerically convergent. The remaining issue is numerical accuracy, in particular in unsteady aerodynamic effects in turbulence response. It is found numerically that if a damping term is added to each of all other equations, numerical convergence is very good; but the flight variables will not vary as much as the data show, as will be illustrated later. To solve this accuracy issue, damping will be added only when it is necessary. It is found numerically that the roll angle (ϕ) tends to have a more negative value than that in the data. Therefore, a term, $-C_1\phi$, is added to both sides of Eq. (8) to cure it. C_1 is assumed to be 0.1. All equations other than Eqs. (2), (3), (8), (11), and (12) are not modified.

Numerical Results

The subject aircraft is a twin-jet transport that encountered a severe clear air turbulence at an altitude of about 33,000 ft. and developed a maximum load factor of 1.75. Based on the FDR data and fuel flow tables in the flight manual, a thrust model is developed [10]. Models for the aerodynamic coefficients are developed in the following form with the fuzzy logic algorithm:

Longitudinal aerodynamics = function($\alpha, \dot{\alpha}, q, k_1, \beta, \delta_e, M, p, \delta_s, \bar{q}$)

Lateral-directional aerodynamics = function($\alpha, \beta, \phi, p, r, k_2, \delta_a, \delta_r, M, \dot{\alpha}, \dot{\beta}$) where k_1 and k_2 are the reduced frequencies to represent the aerodynamic lag effect based on the variation of α and roll angle (ϕ), respectively [8]. The identified aerodynamic

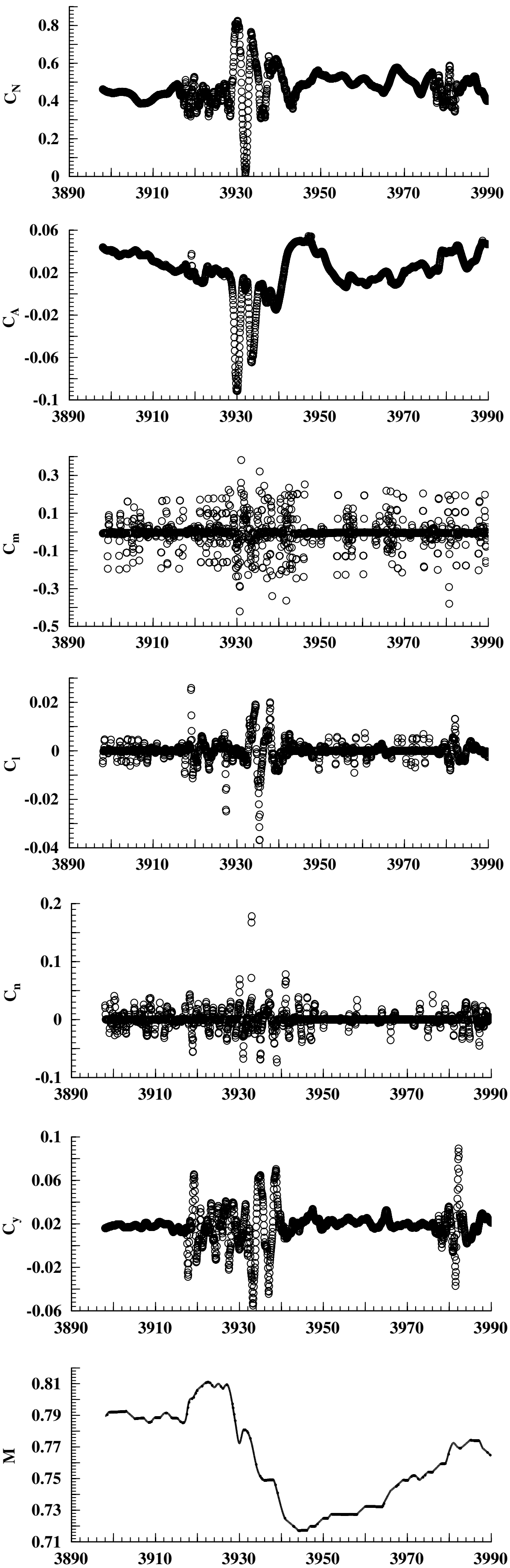

Fig. 1 Data of the aerodynamic coefficients for a twin-jet transport in severe atmospheric turbulence.

coefficients after the bias analysis is performed are presented in Fig. 1. Note that after bias analysis by using the kinematic equations, the flight dynamic equations are employed to determine the aerodynamic coefficients. It is seen from Fig. 1 that there are considerable time variation of all aerodynamic coefficients and data scattering in C_m and C_n, in particular. In a nonlinear simulation, these time variation and scattering are exactly accounted for. To predict the aerodynamic derivatives needed in the present integration method, fuzzy logic modeling method is applied to these data points. The fuzzy logic modeling is formulated in an input/output format. The input consists of the measured plus estimated flight variables as shown above and the output is the aerodynamic coefficients. The estimated variables are those that are not directly measured, such as β, $\mathrm{d}\beta/\mathrm{d}t$, p, r, etc. There are six aerodynamic models for the six aerodynamic coefficients to be determined. With numerous input/output relations available, the fuzzy logic algorithm is applied to train these models by defining the numerical model coefficients to minimize the difference between the data and the prediction of these aerodynamic coefficients in the least square sense, or equivalently to maximize the multiple correlation coefficient. This process is similar to the neural network method. Because the data points are matched only in the least square sense, the aerodynamic models can only predict the average values at every time instant. This is particularly true in predicting the turbulence response. After fuzzy logic

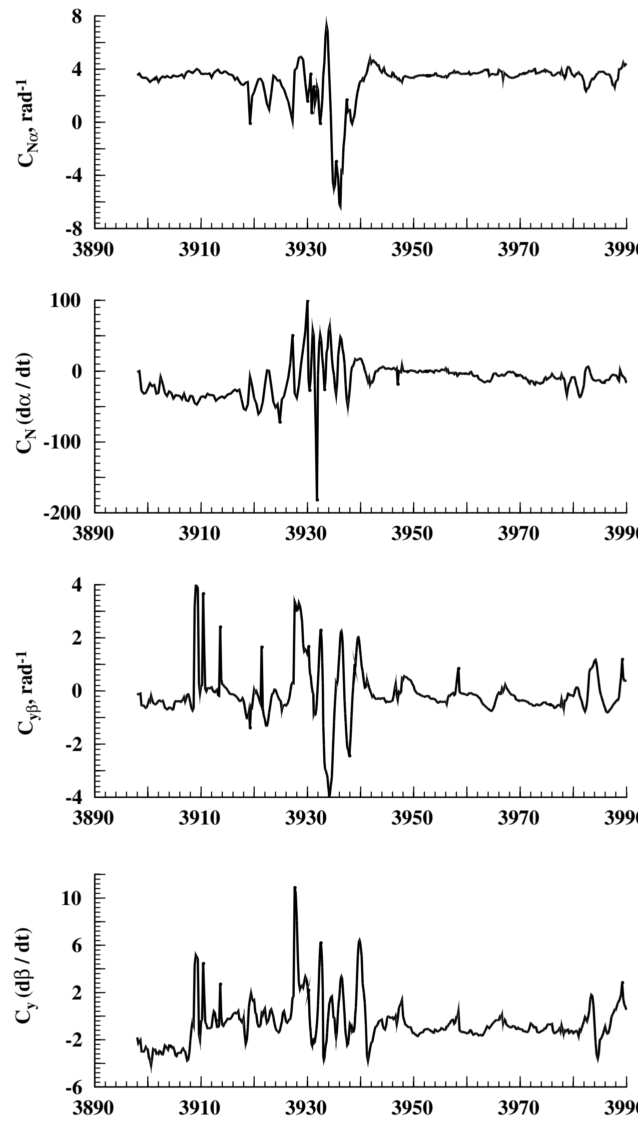

Fig. 2 Aerodynamic derivatives from fuzzy logic models needed in the numerical integration of flight dynamic equations.

modeling, any needed derivatives are estimated from the models by a central difference scheme. In this paper, only the aerodynamic derivatives estimated from the fuzzy logic models, not the aerodynamic coefficients, are employed in the integration of dynamic equations. Those derivatives that are needed in Eqs. (20), (22), (26), and (27) are presented in Fig. 2. All aerodynamic coefficients and the derivatives vary with time considerably in turbulence, as expected.

For trajectory reconstruction and nonlinear simulation, the integration scheme is the fourth-order Runge–Kutta method. There are three methods in flight reconstruction to be compared:

1) Method 1, or "original method with aerodynamic coefficients." This is the original Runge–Kutta forward integration method with only the flight aerodynamic coefficients, not the aerodynamic total forces and moments, plus the engine thrust contribution, being simulated. However, since the tailwind at various altitudes is not known, it is assumed to be a constant value equal to that at the initial altitude. This is to demonstrate the results of inaccurate estimation of dynamic pressure and numerical instability.

2) Method 2, or "original method with total forces and moments." This is the original Runge–Kutta forward integration method with the total aerodynamic forces and moments estimated from the FDR data, including the engine thrust contribution, being simulated. Again, the tailwind is assumed to be a constant value equal to that at the initial altitude.

3) Method 3: This is the present approach by combining method 2 with a damping term in the linear part of the differential equations. The varying tailwind along the flight path is taken to be defined by the FDR data. The variation of tailwind between the initial and ending values along the flight path is about 10%.

Figure 3 shows the main FDR data related to turbulence response. Figure 3a indicates that the original (conventional) method of numerical integration, either with the total forces and moments simulated or not (methods 2 and 1), always yields divergent results in altitude variation over time, and hence cannot generate meaningful data for comparison with the flight data. On the other hand, the present integration method with a damping term can generate very satisfactory results, with the predicted altitude variation being on top of the data. It should be noted that in predicting the altitude change, the w-term in Eq. (12) dominates. Therefore, making α-calculation convergent is very important. Again in all three methods the same aerodynamic coefficients from flight data are employed and only the aerodynamic derivatives needed are obtained from the fuzzy logic models. For the angle of attack due to motion (α_m, Fig. 3b), the present integrated results are more reasonable, having larger differences with the total observed angle of attack during the plunging motion and smaller differences afterwards. Since α_m contributes the most to the total observed angle of attack, the measured loads are mostly from the motion, not the upgust. This is illustrated in Fig. 4. A large positive total α (Fig. 4) coincides with a large positive normal acceleration at about $t = 3930$ s. Similarly, a negative total α at around $t = 3932$ s coincides with a nearly zero normal acceleration.

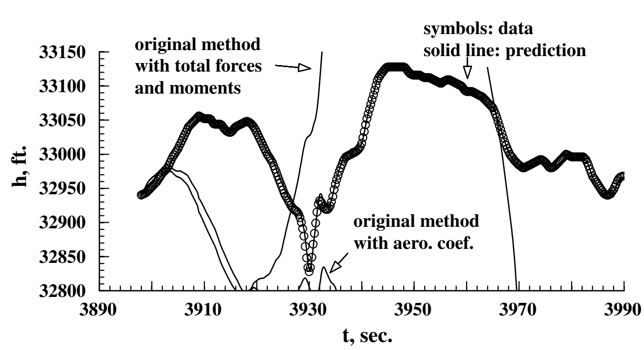

a)

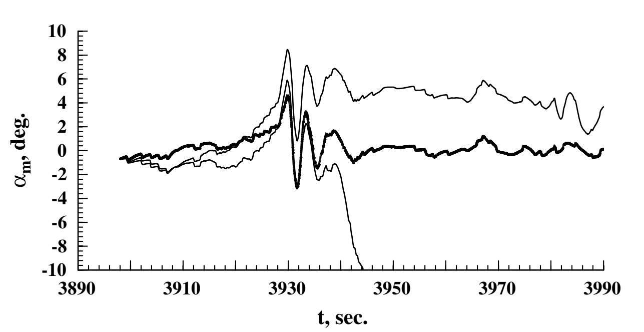

b)

Fig. 3 Comparison of three integration schemes in predicted altitude variation with data.

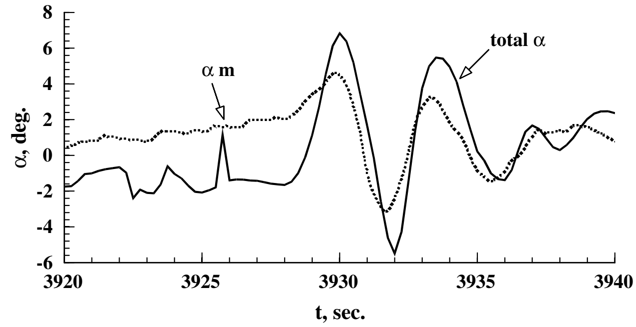

Fig. 4 Comparison of predicted angle of attack due to motion α_m with total α in the data.

The next step to validate an integration scheme is to check on the predicted pitch and roll angles. Both are frequently used by a pilot as cues for proper action. The results of integration with various schemes are presented in Fig. 5. It is seen that if numerical damping is applied to all dynamic equations [Eqs. (1–6)], the results are worse in comparison with data. Some of the dynamic effects from turbulence will not be exhibited properly. Overall, the present scheme with damping in the α- and β-equations appears to be better.

Another flight variable that affects the prediction of the vertical wind in turbulent air is the flight speed [Eq. (19)]. The integrated results are presented in Fig. 6. It is seen that the predicted airspeed, being the aircraft inertial speed reduced by the tailwind, is higher after the severe turbulence encounter which occurred at $t = 3930$ s. Examination of the FDR data also indicates that there was tailwind of about 100 ft/s. Whether the lower indicated airspeed is lower because of the reduced engine thrust caused by turbulence, remains to be investigated. The engine thrust is definitely affected by

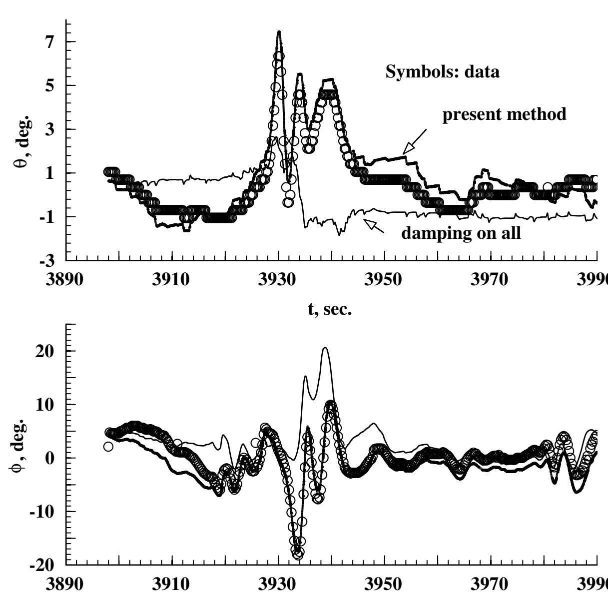

Fig. 5 Comparison of predicted Euler angles with data.

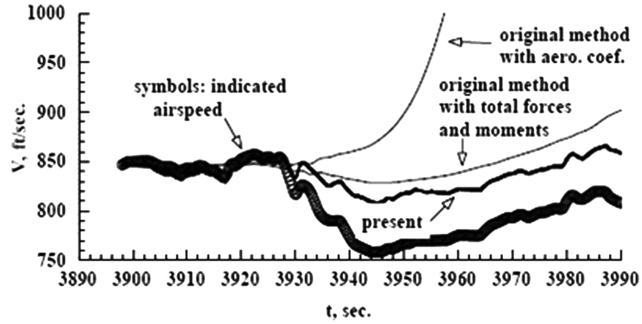

Fig. 6 Comparison of predicted airspeed variation with data.

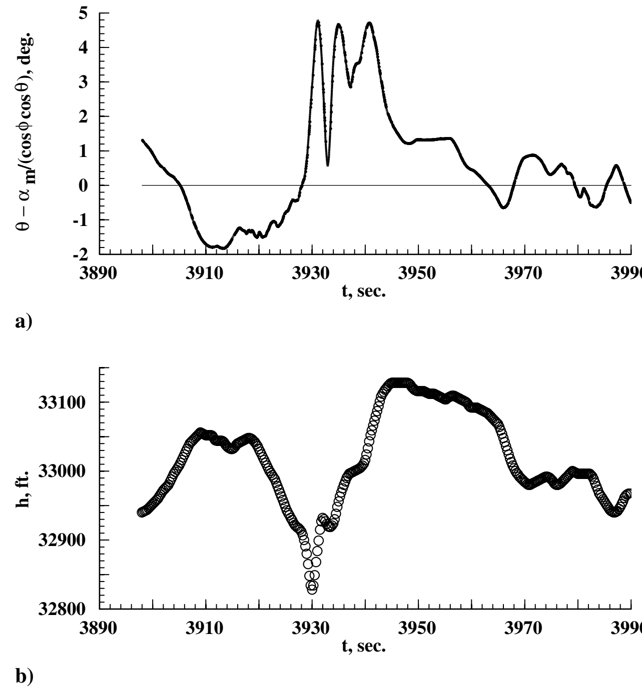

Fig. 8 Estimated flight-path angle based on steady flight concept.

turbulence because the indicated engine pressure ratio dropped to zero at one time during the encounter according to the FDR data (not shown).

Finally, the results for the vertical velocity distribution of atmospheric turbulence are plotted in Fig. 7. It is seen that there are four big jolts –one downwind and 3 upwinds between $t = 3927$ and 3940 s. After that, the upwind and downwind tend to match the variation of the normal acceleration, and represent the more typical "turbulent" air in variation, not the strong gust type. Preceding the first strong upwind, there is downgust between $t = 3916$ and 3929 s to make the total angle of attack negative. Finally, the aircraft plunges downward and the angle of attack increases to generate the highest load at $t = 3930$ s.

One byproduct of the present study is that the following steady flight relations:

$$\frac{\mathrm{d}h}{\mathrm{d}t} = V \sin\gamma \tag{31a}$$

$$\gamma = \theta - \alpha_m/(\cos\theta\cos\phi) \tag{31b}$$

are not valid in unsteady flight. Note that Eq. (31a) is based on earth-fixed axes; while α_m is computed on the body-fixed axes. If they are valid, the sign of γ from both equations should be consistent. The computed results for $\theta - \alpha_m/(\cos\theta\cos\phi)$ are compared with $h(t)$ in Fig. 8. In aircraft performance analysis, γ from Eq. (31a) is equal to the flight-path angle. Therefore, if $\mathrm{d}h/\mathrm{d}t$ is positive, so is the flight-path angle in steady flight. However, in Fig. 8a, it is seen that a positive or negative γ does not always coincide with the sign of $\mathrm{d}h/\mathrm{d}t$ (Fig. 8b). For example, at $t = 3916$ s. $\mathrm{d}h/\mathrm{d}t$ is positive; but $\theta - \alpha_m/(\cos\theta\cos\phi)$ is negative. It is because $(\theta - \alpha_m/(\cos\theta\cos\phi))$ is a fast variable and $h(t)$ is a slow one. A fast variable can oscillate fast locally without affecting the slow one. Conceptually, this phenomenon could be important in that to control plunging, steady flow concept may not be effective. Another application is in UAV flight data analysis. A typical UAV is not equipped with an α-sensor. But α is an important variable in aerodynamics. If it is estimated in accordance with Eqs. (31a) and (31b), it may not be accurate, or even not correct.

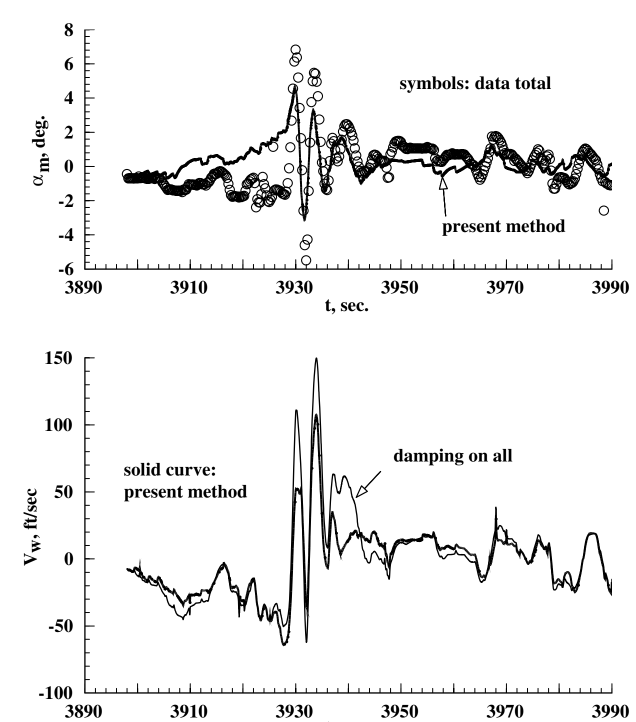

Fig. 7 Predicted vertical wind component of turbulence correlated with motion-induced α.

Conclusions

In this paper, a new integration scheme for the general nonlinear flight dynamic equations with fast-varying aerodynamics was proposed. While successfully performing the trajectory reconstruction and nonlinear simulation, the vertical velocity components of atmospheric turbulence encountered by an aircraft was also estimated. The trajectory was reconstructed by using the aerodynamic derivatives obtained with fuzzy logic models based on a set of FDR data, while the simulation was performed for the flight dynamic equations in six degrees of freedom. The results were used to explain the associated physical phenomena in the plunging motion. The key to success was that the integrated altitude variation matched the data so that the air density was determined more accurately for the aerodynamic forces and moments. Conventional method in integrating the equations in which there was no linear damping terms could not be successful in general. This difficulty has been circumvented by isolating the term associated with the first derivatives to provide the numerical damping. The method developed in this paper could be used in nonlinear simulation to develop control concepts.

References

[1] Kaplan, M. L., Huffman, A. W., Lux, K. M., Cetola, J. D., Charney, J. J., Riordan, A. J., Lin, Y. L., and Waight, K. T., III., "Characterizing the Severe Turbulence Environments Associated with Commercial Aviation Accidents. Part II: Hydrostatic Mesobeta Scale Numerical Simulations of Supergradient Wind Flow and Streamwise A

Geostrophic Frontogenesis," NASA CR-2003-212138, Feb. 2003.
[2] Proctor, F. H., Hamilton, D. W., and Bowles, R. L., "Numerical Study of a Convective Turbulence Encounter," *40th Aerospace Sciences Meeting & Exhibit*, Reno, NV, AIAA Paper 2002-944, Jan. 2002.
[3] Buck, B. K., Bowles, R. L., and Newman, B. A., "Aircraft Acceleration Prediction due to Atmospheric Disturbances with Flight Data Validation," *AIAA Atmospheric Flight Mechanics Conference and Exhibit*, Providence, RI, AIAA Paper 2004-4826, Aug. 2004.
[4] Stewart, Eric C., "Description of a Normal-Force In-Situ Turbulence Algorithm for Airplanes," NASA TM-2003-212666, Dec. 2003.
[5] Buck, W. K., Bowles, R. L., and Newman, B. A., "Aircraft Acceleration Prediction due to Atmospheric Disturbances with Flight Data Validation," AIAA Paper 2004-4826, Aug. 2004.
[6] Stuever, R. A., "Aerodynamic Modeling of an Aircraft in Atmospheric Turbulence and Correlation to Hazard," Ph.D. Dissertation, Univ. of Kansas, 2007.
[7] Wang, Z., Lan, C. E., and Brandon, J. M., "Fuzzy Logic Modeling of Nonlinear Unsteady Aerodynamics," AIAA Paper 98-4351, Aug. 1998.
[8] Wang, Z., Lan, C. E., and Brandon, J. M., "Fuzzy Logic Modeling of Lateral-Directional Unsteady Aerodynamics," AIAA Paper 99-4012, Aug. 1999.
[9] Weng, C-T., and Lan, C. E., *Aerodynamic Analysis of a Landing Transport Airplane in Windshear*, VDM Verlag, Saarbrücken, Germany, May 2008.
[10] Chang, R. C., Yeh, C. E., Lan, C. E., and Guan, M., "Flying Qualities for a Twin-Jet Transport in Severe Atmospheric Turbulence," *Journal of Aircraft*, Vol. 46, No. 5, Sept.–Oct. 2009, pp. 1673–1680. doi:10.2514/1.42408